Supporting Information

Improved electronic coupling in hybrid organic-inorganic nanocomposites employing thiol-functionalized P3HT and non-toxic bismuth sulfide nanocrystals

*Luis Martínez, Sosuke Higuchi, Andrew J MacLachlan, Alexandros Stavrinadis, Nichole Cates, Silke L. Diedenhofen, Maria Bernechea, Sean Sweetnam, Jenny Nelson, Saif A Haque, Keisuke Tajima, Gerasimos Konstantatos**

SI1 – Synthesis and structural characterization of the thiol-functionalized block copolymers

After the addition of the thiol-functionalized monomer, the peak shifts to the high molecular weight without the change of the peak shape in the GPC chart as shown in Figure S1, indicating successful block copolymerization. The GPC analyses of all the polymers show that the M_n was around 20000 with a narrow polydispersity (M_w/M_n) of around 1.1. The ratio of 3-hexyl and 3-(6-bromohexyl) side chains in the copolymers were determined by ^{1}H NMR (see Figure S2 to S7). After the polymers were purified by washing with 5 M HCl solution[4] and Soxhlet extraction with methanol and hexane, bromide groups in the side chain of the diblock copolymers were converted to thioester groups and subsequently to thiol groups by following the reported procedure[5]. The quantitative conversion was confirmed by the complete disappearance of the peak of the methylene proton peaks next to bromine at 3.42 ppm and the appearance of the methylene proton peaks next to thioester group and thiol group respectively at 2.32 ppm and 2.54 ppm, respectively, in ^{1}H NMR spectra (see Figure S3 to S7). Thiol-functionalized P3HT was obtained after the further purification with Soxhlet extraction with methanol and hexane.

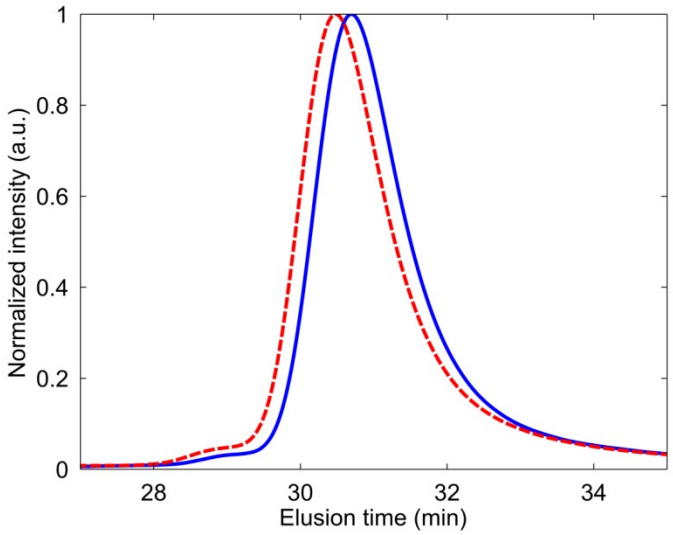

Figure S1 GPC traces of bromide-functionalized diblock copolymers. The solid and broken lines are for P3HTs in the first step and diblock copolymers in the second step, respectively (6%)

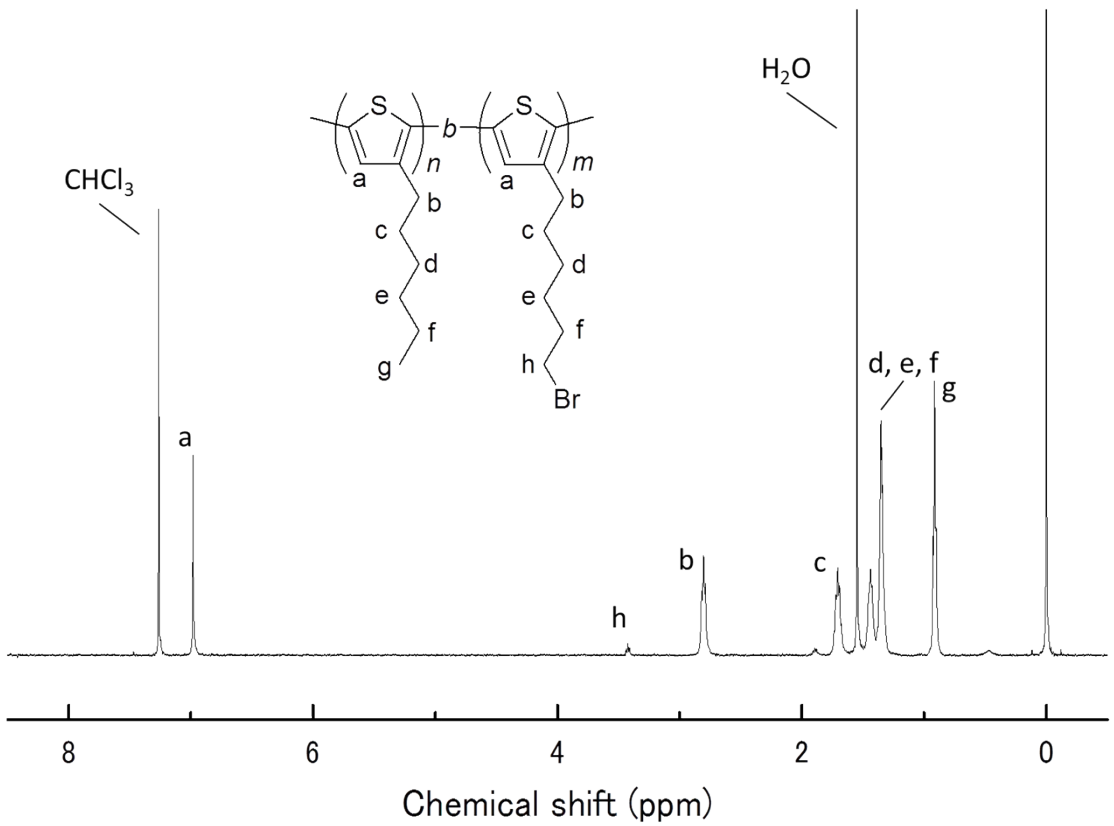

Figure S2 ^{1}H NMR chart of polymer **5** (6 %). Polymer numbering is that of Figure S1.

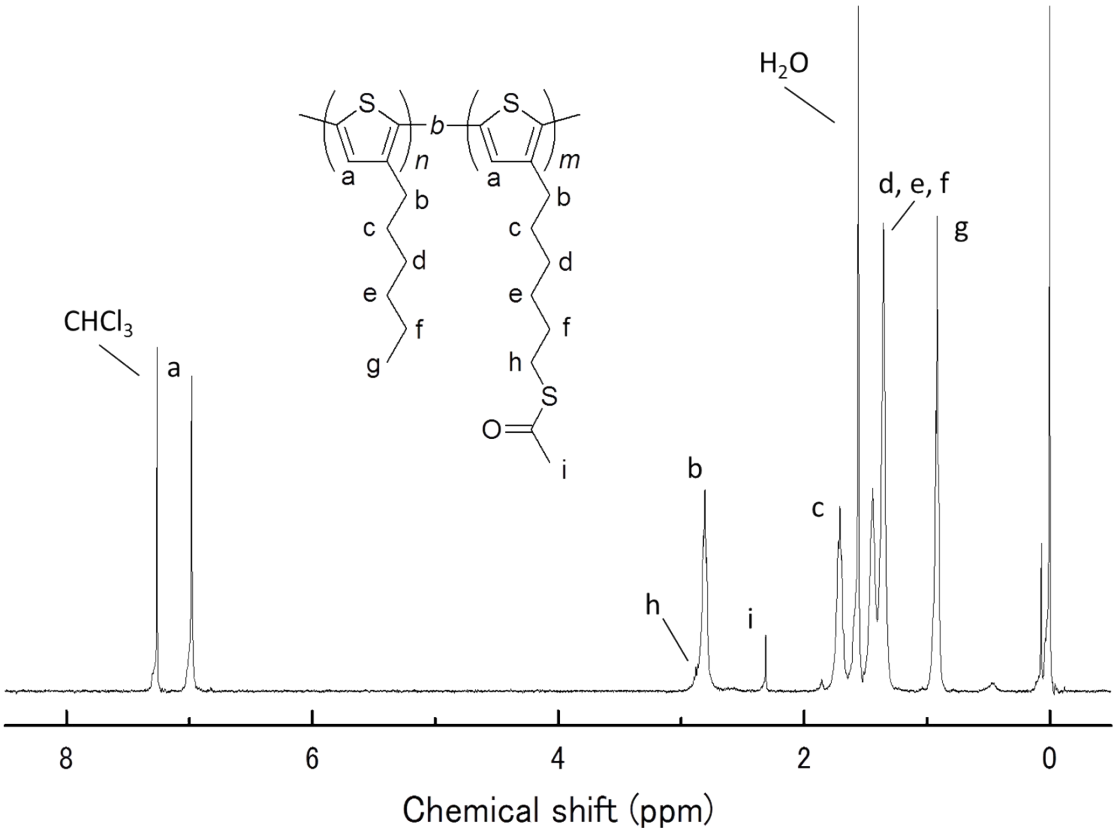

Figure S3 ^{1}H NMRchart of polymer **6** (6 %). Polymer numbering is that of Figure S1.

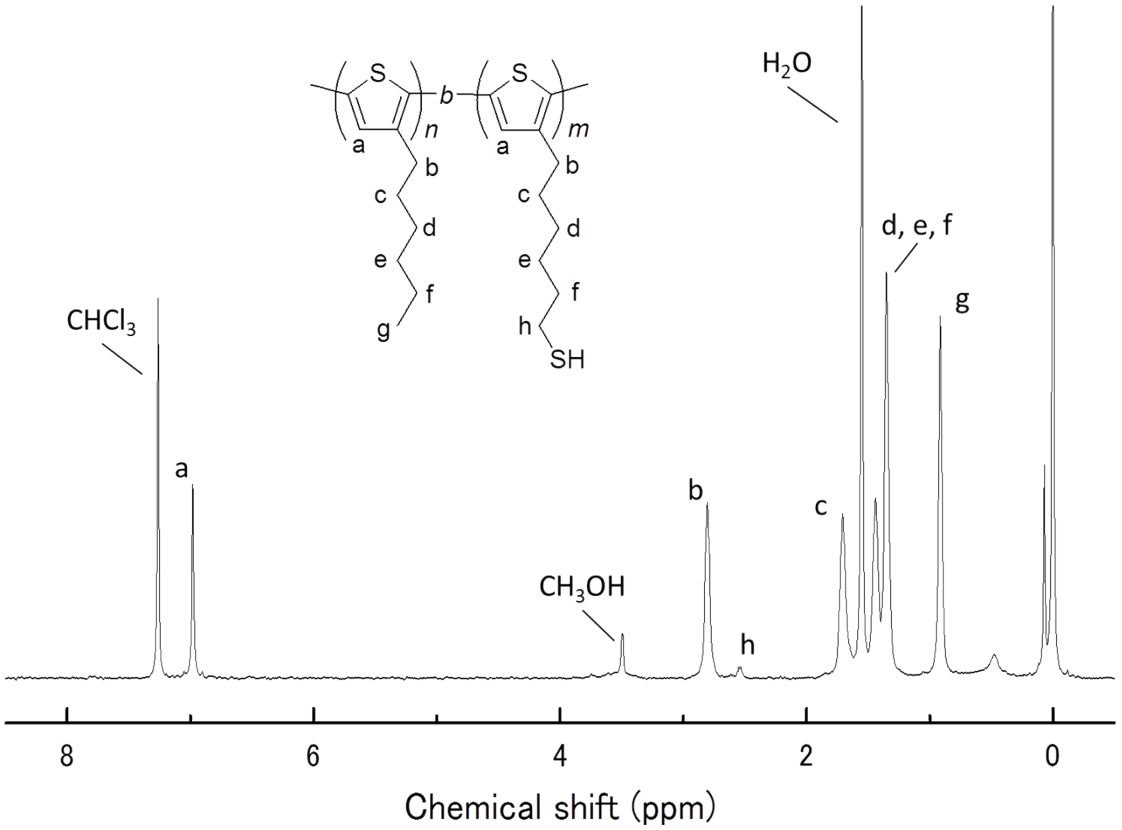

Figure S4 ^{1}H NMR chart of polymer **7** (6 %). Polymer numbering is that of Figure S1.

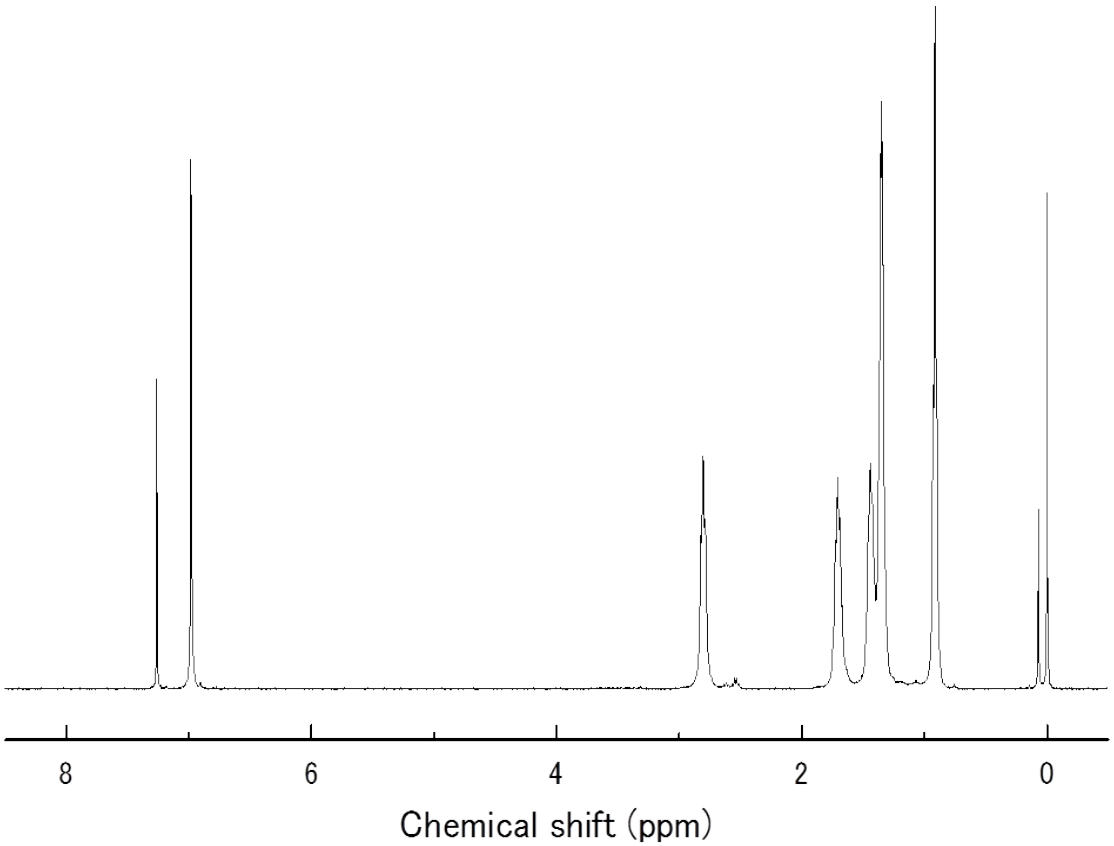

Figure S5 ^{1}H NMR chart of Thiol-functionalized diblock copolymer **7** (4 %). Polymer numbering is that of Figure S1.

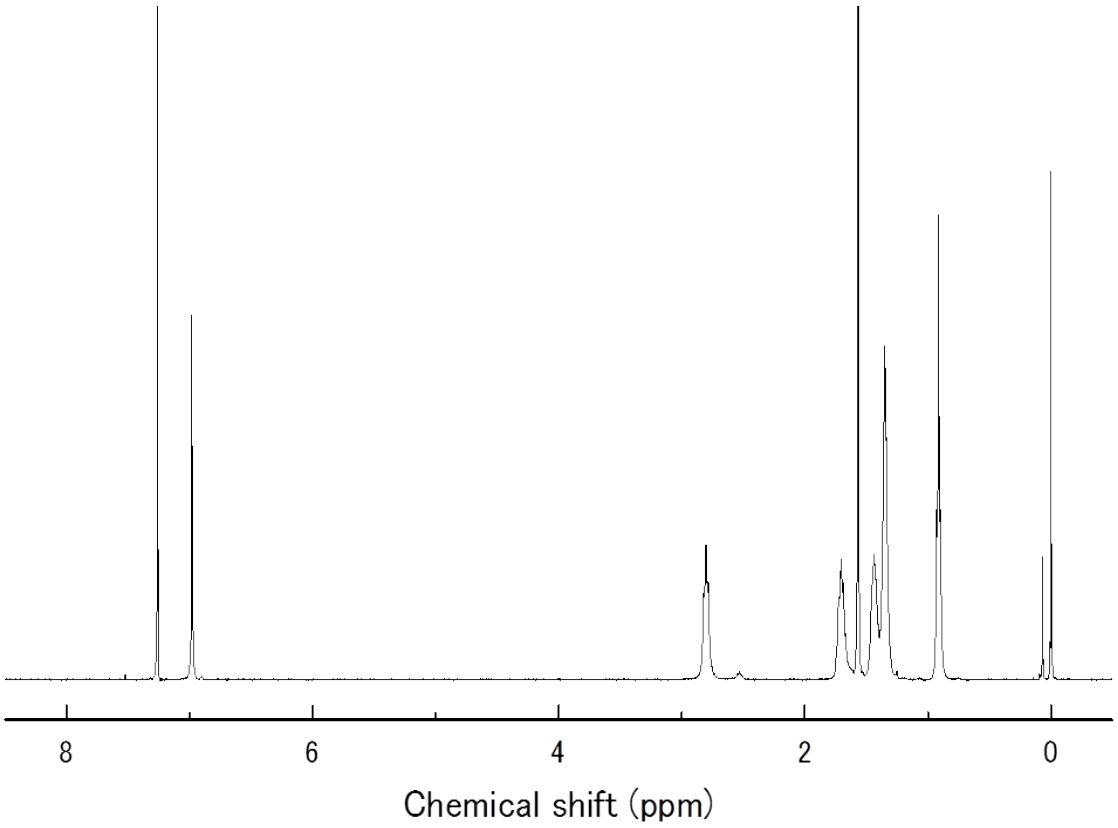

Figure S6 ^{1}H NMR chart of Thiol-functionalized diblock copolymer **7** (1 %). Polymer numbering is that of Figure S1.

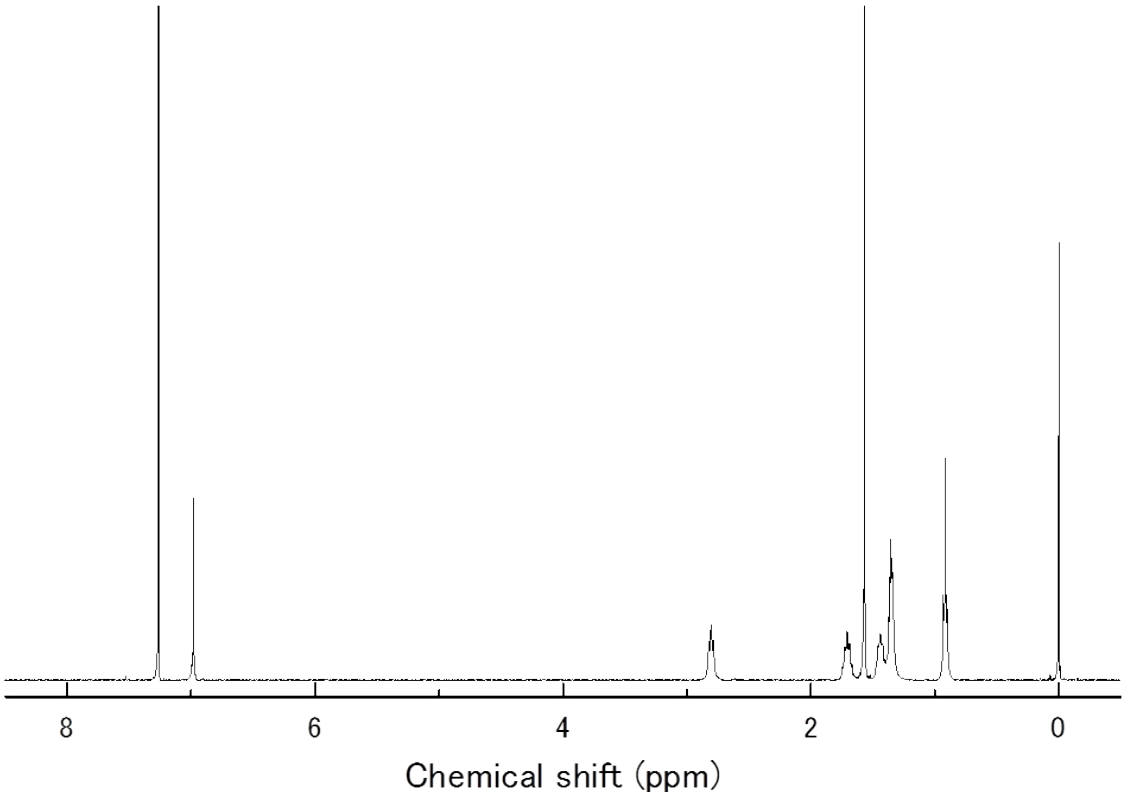

Figure S7 ^{1}H NMR chart of Thiol-functionalized diblock copolymer **7** (<1 %). Polymer numbering is that of Figure S1.

SI 2 – TAS spectra

Transient absorption spectra of P3HT-SH:Bi_2S_3 and P3HT:Bi_2S_3 were obtained after excitation with the laser pulse at 510 nm with a power of 13.27 μJcm^{-2}. The probe light was then changed in wavelength to obtain a photoinduced absorption signal for each wavelength. The points are generated by taking an average of the signal between 1-2 μs.

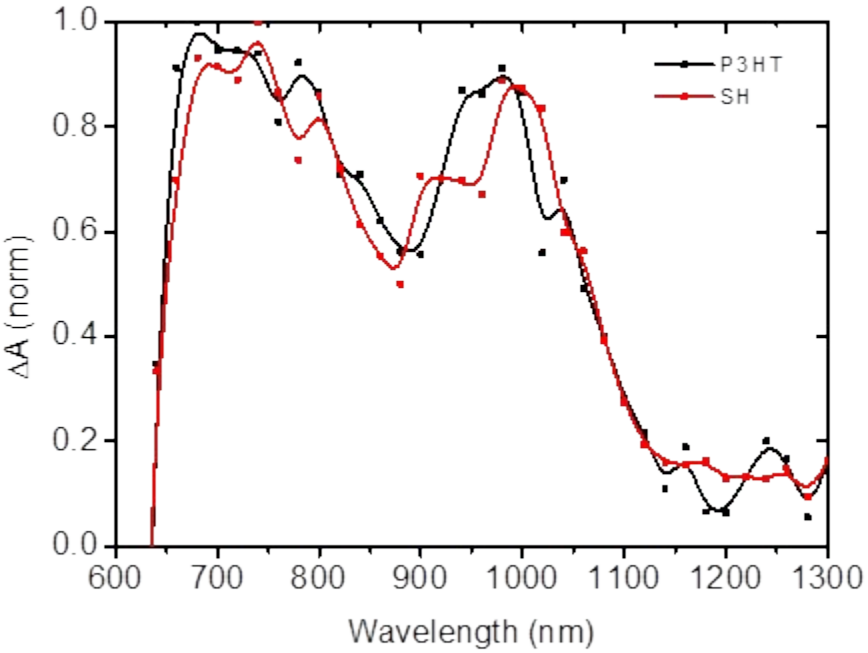

Figure S8 Normalized transient absorption spectra of P3HT (black line) and P3HT-SH (red line).

SI 3 – Photoelectron spectroscopy in air

A RKI AC-2 system was employed to measure the ionization potential of P3HT and P3HT-SH. We observe that P3HT-SH ionization potential energy is approximately 50 meV deeper compared to P3HT.

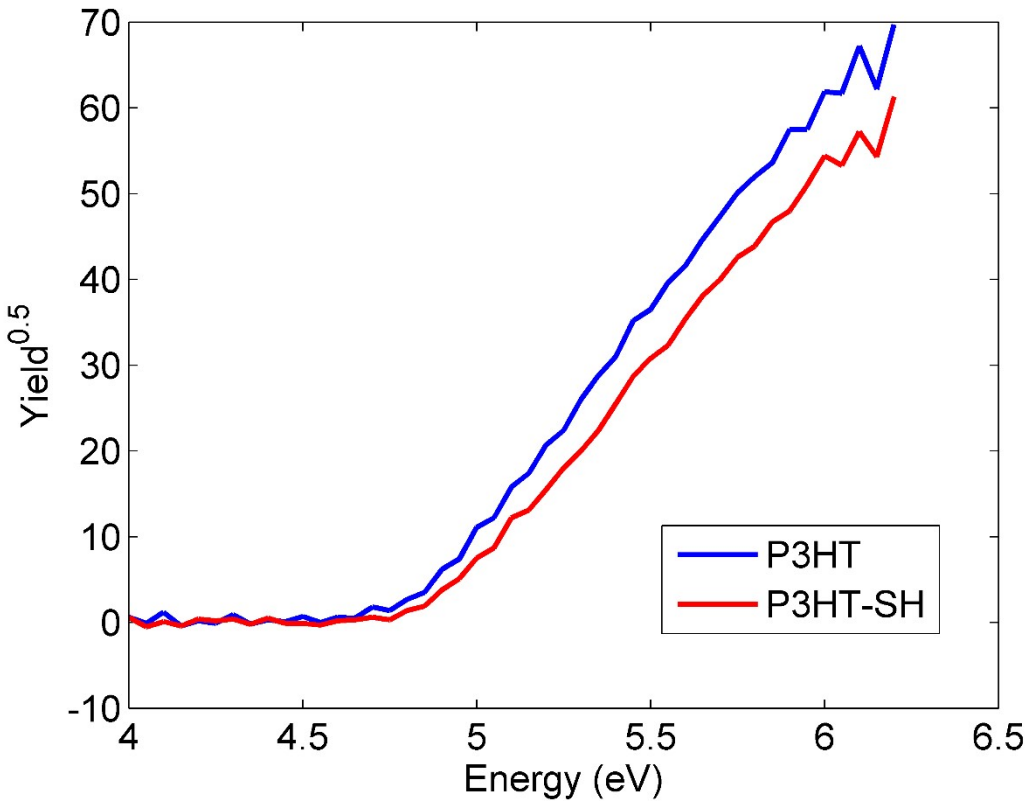

Figure S9 Photoelectron spectroscopy in air of P3HT (blue line) and P3HT-SH (red).

SI 4 – Field Effect Ttransistors (FET)

Bottom gated FET devices were fabricated on silicon substrates coated with 200 nm of thermally grown silicon dioxide. Top gold electrodes were deposited using a shadow mask defining a channel length of 15 µm and width of 1 mm (Ossila), as sketched in Figure S10.

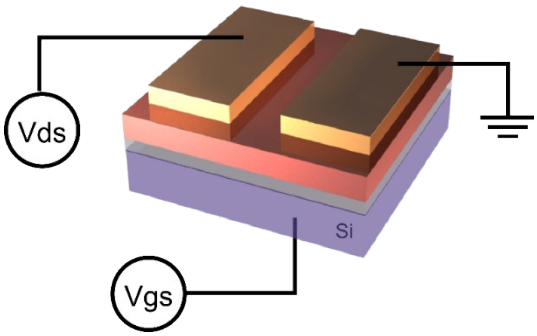

Figure S10 Schematic of the FET.

Current-voltage characteristics were obtained with an Agilent B1500A semiconductor parameter analyzer. Hole mobilities were calculated from the slope of the transconductance (Figure S11) according to the expression:

$$\mu = \frac{L\frac{\partial I_{ds}}{\partial V_{gs}}}{WC_iV_{ds}}$$

Where *L* and *W* stand for the channel length and width, respectively, V_{ds} is the drain-source voltage applied (15 V) and C_i is the capacitance per unit area of the insulator (17 nFcm^{-2}). Calculated hole mobilities are $7 \cdot 10^{-3}$ and 10^{-2} cm^2/Vs for P3HT and P3HT-SH<1%, respectively.

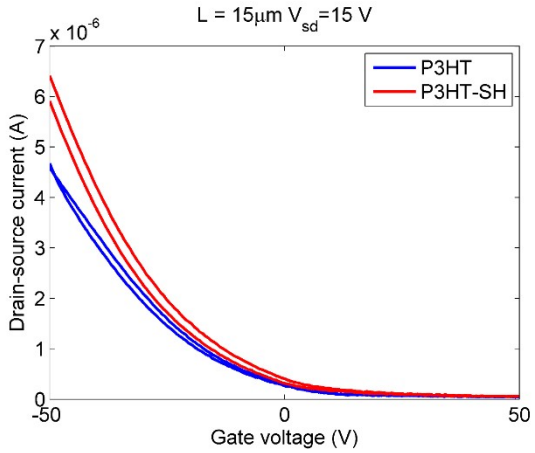

Figure S11 Fitting of the transconductance in field effect transistors (FETs) made of P3HT (blue solid line) and P3HT-SH <1% (red solid line).

SI 5 – Optimization P3HT to P3HT-SH ratio

We fabricated solar cells with the structure ITO/ZnO/BHJ/P3HT/MoO_3/Ag, where BHJ is a mixture of Bi_2S_3 nanocrystals and P3HT and P3HT-SH, at different P3HT to P3HT-SH weight ratio. We aim at identifying an optimal concentration balancing charge transfer between NCs and polymer and electron hopping from NC to NC.

P3HT to P3HT-SH ratio (wt)	Voc (V)	Jsc (mA cm^{-2})	FF (%)	PCE (%)
60:40	0.36	6.5	42	0.97
70:30	0.34	7.6	42	1.1
80:20	0.34	7.1	36	0.87

Table S1 Figures of merit of the hybrid solar cells based on bismuth sulfide and employing different P3HT to functionalized P3HT ratios.

SI 6 – Optimization block copolymer ratio

We fabricated solar cells with the structure ITO/ZnO/BHJ/P3HT/MoO_3/Ag, where BHJ is a mixture of Bi_2S_3 nanocrystals and P3HT and P3HT-SH, employing different block copolymer ratios. The proportion of P3HT to functionalized polymer was kept to 70:30 wt. based on SI5.

Block copolymer ratio	Voc (V)	Jsc (mA cm^{-2})	FF (%)	PCE (%)
<1%	0.34	7.6	42	1.1
1%	0.36	6.3	45	1.02
4%	0.32	6.1	38	0.74

Table S2 Figures of merit of the hybrid solar cells based on bismuth sulfide and employing different bloc copolymer ratios.

SI 7 – Characterization of the bismuth sulfide nanocrystals

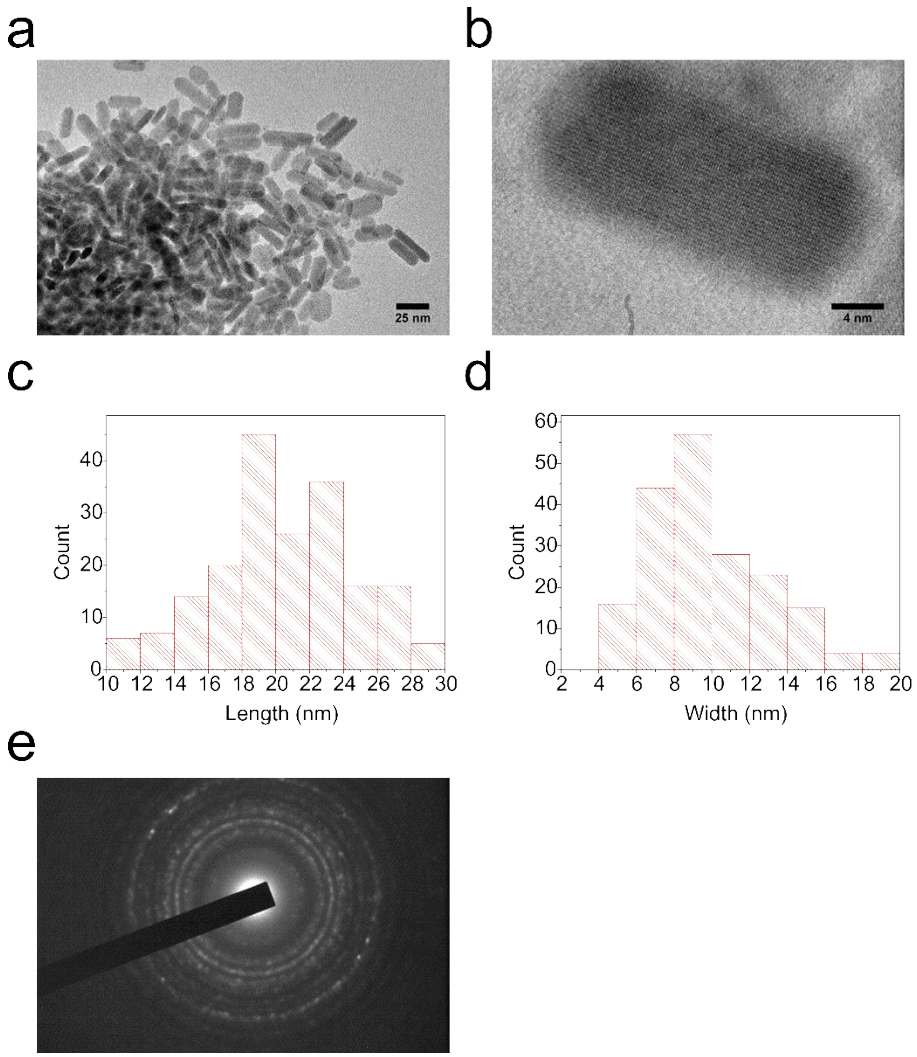

Figure S12 (a,b) TEM micrographs of Bi2S3 nanocrystals revealing a rod-like shape (c, d) size distribution (10x20 nm) (e) X-ray Diffraction pattern of Bi2S3 nanocrystals

References

[1] Miyanishi, S., Zhang, Y., Hashimoto, K., Tajima, K. (2012). Controlled Synthesis of Fullerene-Attached Poly(3-alkylthiophene)- Based Copolymers for Rational Morphological Design in Polymer Photovoltaic Devices. *Macromolecules*, *45*, 6424-6437.

[2] Miyakoshi, R., Yokoyama, A., Yokozawa, T. (2005). Catalyst-Transfer Polycondensation .Mechanism of Ni-Catalyzed Chain-Growth Polymerization Leading to Well-Defined poly(3-hexylthiophene). *Journal of the American Chemical Society*, *127*(6), 17542–17547.

[3] Iovu, M. C., Sheina, E. E., Gil, R. R., McCullough, R. D. (2005). Experimental Evidence for the Quasi-“Living” Nature of the Grignard Metathesis Method for the Synthesis of RegioregularPoly(3-alkylthiophenes). *Macromolecules*, *38*(21), 8649–8656.

[4] Miyakoshi, R., Yokoyama, A., Yokozawa, T. (2004). Synthesis of Poly(3-hexylthiophene) with a Narrower Polydispersity. *Macromolecular Rapid Communications*, *25*(19), 1663–1666.

[5] Zhai, L., Pilston, R. L., Zaiger, K. L., Stokes, K. K., McCullough, R. D. (2003). A simple method to generate side-chain derivatives of regioregular polythiophene via the GRIM metathesis and post-polymerization functionalization. *Macromolecules*, *36*, 61–64.